Chaos, Solitons and Fractals 209 (2026) 118458

Contents lists available at ScienceDirect

Chaos, Solitons and Fractals

journal homepage: www.elsevier.com/locate/chaos

Anomaly detection in directed dynamic graphs using Hermitian Laplacian spectral analysis

Guihai Yu [a,b], Yulei Yue [a,b], Xiaopeng Li [a,b,c,*], Matjaž Perc [d,e,f,g,**]

[a] School of Mathematics and Statistics, Guizhou University of Finance and Economics, Guiyang, Guizhou, 550025, People's Republic of China
[b] School of Big Data Statistics, Guizhou University of Finance and Economics, Guiyang, Guizhou, 550025, People's Republic of China
[c] Guizhou Key Laboratory of Artificial Intelligence and Brain-inspired Computing, Guiyang, Guizhou, 550018, People's Republic of China
[d] Faculty of Natural Sciences and Mathematics, University of Maribor, Koroška cesta 160, Maribor, 2000, Slovenia
[e] Community Healthcare Center Dr. Adolf Drolc Maribor, Vošnjakova ulica 2, Maribor, 2000, Slovenia
[f] Department of Physics, Kyung Hee University, 26 Kyungheedae-ro, Dongdaemun-gu, Seoul, 02447, Republic of Korea
[g] University College, Korea University, 145 Anam-ro, Seongbuk-gu, Seoul, 02841, Republic of Korea

ARTICLE INFO

Keywords:
Directed dynamic graphs
Spectral methods
Anomaly detection
Hermitian Laplacian matrix

ABSTRACT

Dynamic graphs have become an important tool for characterizing interactions among entities and are widely used in fields such as finance, public health, and social network analysis. In many real-world settings, including capital flows, information diffusion, and epidemic spreading, the underlying networks are inherently directed. However, most existing anomaly detection methods for dynamic graphs do not explicitly incorporate edge directionality. Conventional adjacency and Laplacian matrices are not well suited to encoding directional information, which limits their ability to represent directed structures and may reduce detection accuracy. To address this limitation, we propose an anomaly detection method for directed dynamic graphs based on Hermitian Laplacian spectral analysis. The proposed framework constructs a spectral representation that preserves directional information and incorporates a temporal window mechanism to characterize structural variations over time, thereby enabling the identification of anomalous time points. We evaluate the method on synthetic data and on two real-world datasets, namely the UCI Message network and the global vaccine trade network. The results show that the proposed approach outperforms several baseline methods in detecting anomalous time points and more effectively captures anomalies associated with structural changes and directional heterogeneity. These findings indicate that the proposed framework provides both methodological and empirical advances for anomaly detection in directed dynamic graphs, while also offering useful insights into structural perturbations in complex systems.

1. Introduction

In many real-world domains, including finance, economics, sociology, and public health, complex systems are naturally represented as networks that evolve over time. The dynamic networks provide a powerful framework for describing the interactions among and understanding the mechanisms behind complex processes. Within this context, anomaly detection has long been recognized as a fundamental problem in network analysis. Identifying unusual structural patterns in evolving networks is of considerable practical importance and has been widely studied in a variety of application scenarios, including social media security,

* Corresponding author at: School of Big Data Statistics, Guizhou University of Finance and Economics, Guiyang, Guizhou, People's Republic of China.
** Corresponding author at: Faculty of Natural Sciences and Mathematics, University of Maribor, Koroška cesta 160, 2000 Maribor, Slovenia.
E-mail addresses: lxp_392@126.com (X. Li), matjaz.perc@gmail.com (M. Perc).

https://doi.org/10.1016/j.chaos.2026.118458
Received 26 March 2026; Received in revised form 18 April 2026; Accepted 30 April 2026

public health monitoring, computational biology, and the reliable operation of critical infrastructures such as power grids and the Internet of Things [1–7].

The goal of anomaly detection in dynamic graphs is to identify time-varying patterns that deviate significantly from the normal behavior of the network. Because dynamic networks evolve over time, such anomalies are rarely isolated events; instead, they often manifest as abrupt structural changes or shifts in propagation patterns, which may signal the occurrence of important underlying events [8,9]. In financial networks, for example, unusually large unidirectional or asymmetric capital flows may indicate potential fraud or money laundering activities rather than normal market behavior [10,11]. In social networks, messages that spread widely without the usual reciprocal interactions may reveal abnormal dissemination patterns or external manipulation [12,13]. In many of these cases, the abnormal behavior is closely related to the direction of interactions between nodes [14,15]. As a result, capturing directionality becomes essential for understanding and detecting anomalous structural changes.

Despite the increasing interest in anomaly detection for dynamic graphs, the analysis of directed dynamic networks remains challenging. One key difficulty lies in modeling directional structures [16]. In directed networks, interactions between nodes are inherently asymmetric, yet many existing approaches still rely on adjacency matrices or conventional Laplacian matrices that do not explicitly encode edge directionality. Consequently, these methods may fail to capture directional variations in processes such as capital flows, trade interactions, or information diffusion, thereby limiting their ability to detect anomalies accurately. A second challenge arises from the temporal nature of dynamic graphs. Since network structures evolve continuously over time, effective anomaly detection requires methods that can simultaneously capture temporal dependencies while preserving both structural and directional information [17].

To address these challenges, this study proposes a novel anomaly detection framework for directed dynamic graphs based on Hermitian Laplacian spectral analysis. The proposed method, termed H-GAD, introduces a Hermitian adjacency matrix to explicitly encode directional interactions and constructs the corresponding Hermitian Laplacian matrix to characterize global structural properties of the network. Spectral representations are obtained through eigenvalue decomposition, where the dimensionality of the representation is determined adaptively according to the cumulative energy of the spectrum. To further capture temporal variations, a dual-window mechanism combining short-term and long-term sliding windows is employed, with window lengths adaptively adjusted according to the volatility of anomaly scores. This design enables the proposed framework to effectively detect structural anomalies that exhibit both directional and temporal dependencies.

The main contributions of this study can be summarized as follows. First, we propose a Hermitian Laplacian spectral analysis-based approach that explicitly incorporates edge directionality through the construction of a Hermitian adjacency matrix while capturing global topological characteristics via the Hermitian Laplacian matrix. Second, the proposed approach derives spectral representations of graphs via eigenvalue decomposition of the Hermitian Laplacian matrix, where the spectral dimensionality is adaptively determined based on cumulative energy proportion. As a further step, we introduce a temporal modeling strategy that integrates both short-term and long-term sliding windows. By adaptively tuning the window size in response to the fluctuation of anomaly scores, this method is capable of effectively identifying structural anomalies that exhibit directional patterns and temporal dependencies.

2. Related works

2.1. Statistical-based methods for anomaly detection

Anomaly detection research originated in the field of statistics, where it was generally assumed that normal data followed a known distribution. By assessing the deviation of data points from the probability density or central tendency of this distribution, potential anomalies could be identified. Haystack [18] pioneered one of the earliest computer intrusion detection systems based on statistical anomaly detection algorithms. By integrating security policy constraints with models of typical user and group behaviors, it transformed large-scale trace data into summarized anomaly events, thereby addressing the challenge of timely detection of internal intrusions in multi-user computer systems. Bremer [19] reviewed statistical anomaly detection methods developed since 1984, including Gaussian mixture models, regression models, and kernel density estimation (KDE). These approaches are particularly well-suited for numerical data and have been widely applied due to their simplicity and computational efficiency. Basseville et al. [20] further provided detailed descriptions of fundamental algorithms such as control charts, CUSUM procedures, and likelihood ratio tests.

Although early statistical methods played a pivotal role in anomaly detection and established the theoretical foundation for subsequent advances, they face two notable limitations. First, they have difficulties in capturing nonlinear or structural anomalies in complex data. Second, they possess limited capacity to effectively represent node relationships and evolving structures in dynamic graphs. As a result, these methods are not well-suited for anomaly detection in scenarios involving dynamically evolving systems, such as financial and trade networks.

2.2. Machine learning-based methods for anomaly detection

With the rapid development of machine learning, approaches such as proximity measures, clustering analysis, and decision trees have been widely applied to anomaly detection tasks. Proximity-based methods can generally be categorized into density-based and distance-based approaches. Breunig et al. [21] proposed the density-based Local Outlier Factor (LOF) algorithm, which measures the degree of anomaly by evaluating the local density deviation of a data point relative to its neighbors. Edwin et al. [22] introduced

the distance-based DB-outliers algorithm, which employs multidimensional distance metrics to improve the efficiency of anomaly detection in high-dimensional and large-scale datasets. Although proximity-based methods are effective in identifying local outliers, they are often sensitive to parameter settings and incur considerable computational cost. More importantly, these methods focus on point-wise characteristics and lack the ability to capture global structural information, particularly graph topology, which limits their effectiveness in detecting anomalies rooted in relational structures.

Clustering-based methods have also been widely adopted for anomaly detection. Representative approaches include partitioning clustering [23,24], hierarchical clustering [25–27], density-based clustering [28], and grid-based clustering [29], where anomalies are typically identified as points located far from cluster centers, isolated subclusters, or low-density regions. While clustering methods do not require labeled data and can reveal latent structures within datasets, they are highly sensitive to parameter choices and often perform poorly in high-dimensional spaces. Moreover, most clustering algorithms are designed for static data and have limited ability to capture the temporal evolution of complex networks, which restricts their applicability to dynamic graph scenarios.

Decision tree-based approaches are also widely used in anomaly detection due to their simplicity and interpretability. Breiman et al. [30] proposed the Random Forest method, which improves the identification of minority anomalous samples by aggregating multiple decision trees. Markou and Singh [31] provided a comprehensive survey of novelty detection methods, highlighting the role of classification-based approaches such as decision trees. Liu et al. [32] later introduced the Isolation Forest algorithm, which isolates anomalous samples through random feature selection and recursive partitioning. Owing to its scalability and efficiency, Isolation Forest has become one of the most widely used algorithms for anomaly detection. Nevertheless, decision tree-based methods typically rely on labeled data or threshold settings and have limited ability to model structural relationships and temporal dependencies, which constrains their application in dynamic graph analysis.

2.3. Tensor decomposition-based methods for anomaly detection

In anomaly detection tasks, although traditional machine learning methods have been extensively studied, they often exhibit limited capability in capturing complex inter-node dependencies and temporal evolution patterns, especially in multidimensional dynamic systems such as social, financial, and trade networks. Statistical modeling approaches that explicitly exploit multi-way structural and temporal information have therefore attracted increasing attention. Among them, tensor decomposition provides a powerful statistical framework for modeling dynamic graphs by jointly representing node, relational, and temporal dimensions within a unified high-order tensor structure. By decomposing such tensors, latent low-rank structures and statistically significant deviations can be revealed, enabling the identification of dynamic anomalous behaviors. Owing to its effectiveness in modeling complex dependencies and high-dimensional dynamics, tensor decomposition has become an important class of statistical-based methods for anomaly detection in dynamic networks.

Koutra et al. [33] proposed the TENSORSPLAT method, which formulates dynamic graphs and their multimodal attributes as high-order tensors and applies PARAFAC decomposition to extract latent low-rank components for anomaly detection. Departing from conventional adjacency-matrix-based representations, TENSORSPLAT jointly incorporates node information, relational attributes, and temporal dynamics into a unified statistical model. Anomalous events and long-term behavioral changes are detected by analyzing statistically significant fluctuations of latent factors along the temporal dimension. Due to its systematic characterization of anomalous patterns under a decomposition-based statistical framework, TENSORSPLAT has become a representative and influential approach in the literature on statistical-based anomaly detection for dynamic graphs.

2.4. Spectral-based methods for anomaly detection

Although tensor decomposition can capture latent patterns in multidimensional dynamic networks, it remains limited in characterizing the global topological structure of graphs. To better model the structural properties of dynamic networks, spectral-based anomaly detection methods have gradually emerged as an important research direction.

Ranshous et al. [4] provided a comprehensive survey of anomaly detection in dynamic graphs, categorizing existing approaches into several main groups. Many of these methods rely on discriminative techniques such as thresholds, support vector machines (SVM), or local outlier factor (LOF) applied to graph-derived features. However, most of these approaches focus on undirected graphs or static snapshots and lack dedicated frameworks for directed dynamic networks or directional spectral features. Koutra et al. [34] proposed DeltaCon, which measures structural similarity between graphs by computing node affinity, enabling efficient graph comparison. Nevertheless, this method primarily compares individual graph snapshots and does not explicitly model temporal evolution, which limits its ability to detect gradual structural changes in dynamic networks. Huang et al. [35] were among the first to apply Laplacian spectral analysis to change point and event detection in dynamic graphs. Their approach performs singular value decomposition (SVD) on the Laplacian matrix to obtain low-dimensional graph embeddings and employs a dual sliding-window mechanism to model temporal dependencies. Although this method can be applied to directed graphs, the constructed Laplacian matrix does not explicitly distinguish between in-degree and out-degree information. In many real-world systems, such as trade networks, information diffusion networks, and epidemic transmission networks, directionality plays a critical role. Simplifying these networks as undirected graphs or symmetrizing the adjacency matrix may therefore lead to the loss of important structural information.

Building upon this, Luo et al. [36] proposed a Fréchet statistics-based change point detection method, which characterizes the temporal evolution of network structure through statistical analysis of the Laplacian matrix within sliding windows. While this

approach effectively captures structural changes over time, it still relies on the classical Laplacian matrix and does not explicitly represent directional information. Moreover, repeated spectral decompositions introduce additional computational overhead.

Collectively, spectral methods provide significant advantages in capturing structural characteristics of graphs and have become an increasingly important tool for anomaly detection in dynamic networks. However, most existing studies focus on undirected graphs, and research on directed dynamic networks remains relatively limited, particularly methods capable of explicitly modeling edge directionality. Motivated by these limitations, we propose a Hermitian Laplacian-based anomaly detection framework for directed dynamic graphs. By leveraging the Hermitian Laplacian matrix, the proposed approach provides a spectral representation that preserves directional information and captures the temporal evolution of network structure.

3. Theoretical foundations

3.1. Definition of directed dynamic graphs

In practical applications, many relationships exhibit not only dynamic characteristics that evolve over time but also explicit directionality, such as information dissemination, fund transfers, and logistics flows. To characterize such graph structures that possess both temporal and directional properties, we introduce the definition of a directed dynamic graph:

A directed dynamic graph over the time interval $\{1, 2, \dots, T\}$ can be represented as a sequence of graphs $G = \{G_1, G_2, \dots, G_T\}$, where each snapshot $G_t = (V_t, E_t)$ describes the network structure at time t. Here, V_t denotes the set of nodes, and $E_t \subseteq V_t \times V_t \times \mathbb{R}_+$ denotes the set of directed weighted edges. Each edge $(i, j, w_{ij}) \in E_t$ represents a directed edge from node i to node j with weight $w_{ij} \in \mathbb{R}_+$. For unweighted graphs, we set $w_{ij} = 1$.

We use the adjacency matrix $A_t \in \mathbb{R}^{n\times n}$ to denote each graph snapshot, where $A_t(i, j) = w_{ij}$ denotes the weight of the directed edge from node i to node j, or 0 if the edge does not exist. This graph sequence describes the evolution of the network structure and its directional relationships over time, and is the central object of study for the anomaly detection task in this paper.

3.2. Hermitian adjacency matrix and Hermitian Laplacian matrix

To more effectively represent edge directionality in directed graphs and enable anomaly detection based on spectral characteristics, this study employs the Hermitian adjacency matrix [37,38] and the associated Hermitian Laplacian matrix [39] as matrix representations of graph structural properties. From the perspective of spectral analysis, these matrices capture the directional structural information of directed dynamic graphs, while the temporal evolution of their eigenvalues is exploited to detect potential anomalous events.

Hermitian adjacency matrix. Let $G = (V, E)$ be a directed graph with vertex set V and edge set $E \subseteq V \times V$. The Hermitian adjacency matrix $H = [H_{uv}] \in \mathbb{C}^{n\times n}$ is defined as follows:

If there exists an edge $u \to v$, then $H_{uv} = i$; if there exists an edge $v \to u$, then $H_{uv} = -i$. If the graph is weighted and the weight of edge $u \to v$ is $w_{uv} \in \mathbb{R}$, then $H_{uv} = (w_{uv} - w_{vu})i$. If no edge exists between u and v, then $H_{uv} = 0$.

This definition satisfies the Hermitian property, $H = H^*$, ensuring that all eigenvalues are real and thus enabling effective spectral analysis [40]. By incorporating the imaginary unit to encode edge directions, the matrix explicitly distinguishes between in-degree and out-degree, thereby providing essential structural support for modeling directed graphs.

Hermitian Laplacian matrix. On the basis of the Hermitian adjacency matrix, the Hermitian Laplacian matrix $L \in \mathbb{C}^{n\times n}$ is further defined as:

$$L = D - H \tag{1}$$

where $D = \mathrm{diag}(d_1, d_2, \dots, d_n)$ is the degree matrix, and each d_i denotes the total edge-weight degree of node v_i, given by

$$d_i = \sum_{j=1}^{n} |H_{ij}| \tag{2}$$

The Hermitian Laplacian matrix preserves the classical form of the traditional graph Laplacian while enhancing the ability to characterize directional perturbations, as it is constructed from the Hermitian adjacency matrix. It provides two core advantages. First, it provides directional expressiveness by using the imaginary unit to encode edge directionality and preserve structural differences between in-degree and out-degree. Second, it exhibits favorable spectral properties: since L is Hermitian, all its eigenvalues are real, enabling stable spectral embeddings and reliable anomaly detection.

In summary, the Hermitian adjacency matrix serves as the fundamental representation for encoding directional information, while the Hermitian Laplacian matrix integrates degree information to strengthen the characterization of structural perturbations.

3.3. Anomaly detection

Anomaly detection can generally be divided into change-point detection and event detection. Change-point detection aims to identify moments of abrupt global structural shifts in a network, such as community merging, splitting, or sudden density variations [40,41]. After a change point occurs, it is assumed that the generative process of the underlying dynamic network has undergone a significant transformation, with the parameters of the generative model experiencing drastic changes. In other words, the generative mechanism of the graph differs substantially before and after the change point [42]. In contrast, event detection

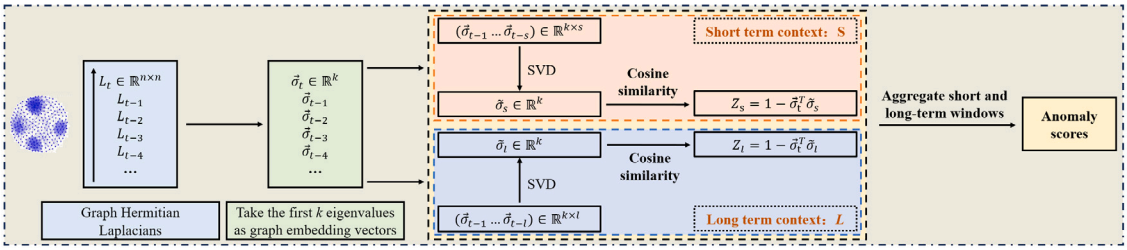

Fig. 1. Flowchart of the proposed H-GAD framework, which performs anomaly detection in directed dynamic graphs by encoding directed structures via a Hermitian adjacency matrix, applying spectral decomposition with adaptively determined dimensionality, and using a dual-window scheme with adaptive window lengths to capture temporal variations.

focuses on localized and instantaneous anomalous activities, such as unusually high activity levels of individual nodes or the sudden emergence of new connections. An event is defined as a transient deviation in network behavior at a specific time point, after which the network returns to its normal state. Examples include traffic disruptions caused by sudden incidents or increased activity at the beginning of a new academic term [43].

The core objective of anomaly detection is to identify abnormal variations in a given graph snapshot G_t relative to the expected normal behavior. To this end, we introduce an anomaly scoring function $f : \mathcal{G} \to \mathbb{R}$, which assigns a score to each graph snapshot. Specifically, let G_N denote the global normal behavior of the network, and G_W denote the short-term behavior observed within a recent time window W.

Anomaly detection can be categorized into two cases. In the case of global anomaly detection, a graph G_t is regarded as anomalous if its score deviates substantially from that of the global normal graph G_N, i.e., $|f(G_t) - f(G_N)| > \delta$. In the case of local anomaly detection, a graph G_t is regarded as locally anomalous if its score deviates substantially from that of the short-term window G_W, i.e., $|f(G_t) - f(G_W)| > \epsilon$.

Here δ and ϵ are predefined thresholds that determine the magnitude of score deviations considered anomalous. An effective anomaly scoring function should possess strong discriminative capability, allowing for a clear separation between normal and abnormal graphs. Moreover, the anomaly score should scale with the severity of the abnormality, reflecting the degree of deviation from expected behavior.

4. Hermitian Laplacian-based anomaly detection

To effectively identify anomalous nodes or events in directed dynamic networks, this study proposes H-GAD, a Hermitian Laplacian spectral analysis-based anomaly detection method for directed graphs. The core idea is to exploit the spectral symmetry and real-valued eigenproperties of Hermitian matrices when modeling directed graphs. By embedding directed edge relationships into the adjacency matrix, a Laplacian representation that explicitly preserves directional information is constructed. This representation enables the extraction of structural variation features from the evolving sequence of graphs over time.

The typical or normal behavior of a graph is characterized by a sequence of vectors composed of the eigenvalues at each time step. By integrating a sliding window mechanism, the method jointly captures both short-term dependencies and long-term evolutionary trends, thereby modeling global structural evolution as well as localized perturbation patterns. Anomalies are then detected by quantifying deviations between the current behavior vector and the normal behavior vector. Through this design, H-GAD achieves efficient detection of anomalies in directed dynamic graphs by simultaneously accounting for temporal evolution, structural variations, and directionality. The overall workflow of the H-GAD framework is illustrated in Fig. 1.

4.1. Spectral properties and representation of the Hermitian Laplacian matrix

Spectral analysis has been widely used for anomaly detection in dynamic graphs, as it captures global structural characteristics and their temporal evolution. For directed networks, the Hermitian Laplacian matrix provides a spectral representation that preserves edge orientation while maintaining desirable mathematical properties.

Let L denote the Hermitian Laplacian matrix. Since L is Hermitian, its eigenvalues are real and the matrix admits the spectral decomposition

$$L = U \Lambda U^*, \tag{3}$$

where U is a unitary matrix whose columns correspond to eigenvectors and Λ is a diagonal matrix containing the associated eigenvalues.

These properties make the Hermitian Laplacian matrix particularly suitable for analyzing directed graphs. First, the eigenvalues of L are real [39,44] and can be ordered as

$$\lambda_1 \geq \lambda_2 \geq \cdots \geq \lambda_n \geq 0. \tag{4}$$

The ordered spectrum provides a stable basis for characterizing the structural state of the network, while abrupt variations in the eigenvalue sequence may indicate structural anomalies over time. Second, the Hermitian Laplacian matrix inherits directional information from the Hermitian adjacency matrix and is therefore sensitive to asymmetric in–out degree structures [38,45]. This property enables the spectral representation to capture directional perturbations that cannot be revealed by traditional Laplacian matrices constructed for undirected graphs.

Based on these properties, each graph snapshot in the dynamic network is represented by the leading k eigenvalues of the Hermitian Laplacian matrix. The resulting k-dimensional spectral feature vector provides a compact description of the global network structure while reducing the influence of local noise [46]. By tracking the evolution of these spectral features across time, structural deviations in the dynamic graph can be effectively identified.

In summary, the Hermitian Laplacian spectrum provides a natural representation for directed dynamic graphs by preserving directional information while capturing global structural variations. However, the effectiveness of spectral representations depends on the number of eigenvalues used to construct the spectral feature sequence. Existing methods, such as LAD [35], typically adopt a fixed spectral dimensionality, ignoring variations in spectral complexity across time, which may lead to information loss or noise redundancy. To address this limitation, an adaptive dimensionality selection mechanism based on cumulative spectral energy is introduced.

4.2. Adaptive eigenvalue selection based on a cumulative energy threshold

In spectral-based anomaly detection for directed dynamic graphs, the eigenvalues of the Hermitian Laplacian matrix are typically sorted in descending order, where leading eigenvalues capture the dominant structural characteristics of the network, while smaller eigenvalues often correspond to local perturbations or noise. Selecting an appropriate number of eigenvalues k for spectral representation is therefore critical for balancing structural expressiveness and robustness. However, most existing methods employ a fixed k, which fails to account for variations in spectral complexity across different snapshots of dynamic graphs.

To overcome these limitations, this paper proposes an adaptive feature dimensionality selection mechanism based on cumulative spectral energy proportion, which is inspired by the cumulative explained variance criterion in principal component analysis (PCA) [47,48]. Specifically, for each time step t, eigenvalue decomposition of the Hermitian Laplacian matrix produces an ordered sequence $\{\lambda_1^t, \lambda_2^t, \ldots, \lambda_n^t\}$. The cumulative spectral energy ratio is defined as

$$E_k^t = \frac{\sum_{i=1}^{k} (\lambda_i^t)^2}{\sum_{i=1}^{n} (\lambda_i^t)^2}, \tag{5}$$

where $(\lambda_i^t)^2$ represents the spectral energy contribution of the ith eigenvalue. To obtain a stable estimate across time, the cumulative energy curves are averaged over all T snapshots,

$$\bar{E}_k = \frac{1}{T} \sum_{t=1}^{T} E_k^t. \tag{6}$$

The final spectral dimensionality is determined as the smallest k satisfying

$$k^* = \min\{k \mid \bar{E}_k \geq \tau\}, \tag{7}$$

where τ denotes the energy coverage threshold. Following the sensitivity analysis in Section 5.4, τ is set to 0.95 in our experiments.

4.3. Construction of the normal behavior vector and anomaly scoring function

4.3.1. Construction of the normal behavior vector

In anomaly detection tasks, we identify anomalous time points in directed dynamic graphs by measuring deviations between the current behavior vector and the normal behavior vector, making it crucial to evaluate whether the current graph state departs from normal behavior. To this end, we adopt the concept of a normal behavior vector as introduced in [49]. Following the approach proposed in [35], a normal behavior vector is extracted from the spectral representations of the previous l graph snapshots. Differing from the original method, we base our feature extraction on the Hermitian Laplacian matrix at each time step, from which the first k eigenvalues are taken to form a spectral embedding vector of length k. The spectral vectors from the l snapshots are then assembled into a $k \times l$ context matrix C:

$$C = \begin{bmatrix} \vec{\sigma}_{t-l,1} & \cdots & \vec{\sigma}_{t-1,1} \\ \vdots & \ddots & \vdots \\ \vec{\sigma}_{t-l,k} & \cdots & \vec{\sigma}_{t-1,k} \end{bmatrix} \tag{8}$$

To eliminate the influence of varying scales, we first normalize each spectral vector to unit length using the L_2 norm. Subsequently, singular value decomposition (SVD) [50] is applied to the context matrix, yielding $C = U \Sigma V^T$. The first left singular vector in U is then regarded as the normal behavior vector for the current sliding window, denoted as $\tilde{\sigma}_t$.

4.3.2. Definition of the anomaly scoring function

After obtaining the normal behavior vector, we adopt the Z-score as the anomaly scoring function proposed in [49] to quantify the deviation between the low-dimensional embedding of the current graph and its normal behavior. This scoring mechanism provides an effective characterization of structural deviations and offers a robust quantitative basis for anomaly identification. Let $\tilde{\sigma}_t$ denote the normal behavior vector constructed from the sliding window, and $\vec{\sigma}_t$ represent the spectral feature vector at the current time step. Both vectors are normalized to unit length. On this basis, the Z-score is employed to measure their discrepancy, and its mathematical formulation is given as follows:

$$Z = 1 - \frac{\vec{\sigma}_t^{\,T}\tilde{\sigma}_t}{\|\vec{\sigma}_t\|_2\,\|\tilde{\sigma}_t\|_2} = 1 - \vec{\sigma}_t^{\,T}\tilde{\sigma}_t = 1 - \cos\theta \tag{9}$$

where $\cos\theta$ denotes the cosine similarity between $\vec{\sigma}_t^{\,T}$ and $\tilde{\sigma}_t$. When there exists a significant discrepancy between the normal behavior vector and the current behavior vector, $\cos\theta$ approaches 0, and the corresponding Z-score tends toward 1, indicating a higher likelihood that the current time step is anomalous. Based on the short-term and long-term normal behavior vectors $\tilde{\sigma}_s$ and $\tilde{\sigma}_l$ obtained in Section 4.3.1, their cosine similarities with the current spectral vector are computed to yield the short-term and long-term anomaly scores, Z_s and Z_l.

To provide a more intuitive understanding of the dual-window mechanism, we explain its practical role in capturing temporal dynamics. In real-world dynamic networks, structural changes often occur at different temporal scales, making it difficult for a single time window to effectively capture both abrupt and gradual variations. The short-term window primarily reflects recent network behavior and is sensitive to sudden structural disruptions, such as rapid changes in connectivity or local interaction patterns. In contrast, the long-term window captures more stable historical trends and is better suited for identifying gradual structural evolution over time.

For example, in a traffic network, a sudden incident such as an accident may lead to an immediate redistribution of traffic flows, which can be effectively detected by the short-term window. Meanwhile, long-term changes, such as seasonal travel patterns or policy-driven shifts in mobility, are more accurately captured by the long-term window. By combining these two temporal perspectives, the proposed framework can effectively distinguish between transient fluctuations and persistent structural changes, thereby improving both the robustness and interpretability of anomaly detection.

4.4. Adaptive sliding window adjustment mechanism based on anomaly score volatility

After constructing the short-term and long-term context matrices, singular value decomposition (SVD) is applied to obtain the corresponding normal behavior vectors, denoted as $\tilde{\sigma}_l$ and $\tilde{\sigma}_s$. At each time step, the current behavior vector is compared with these reference vectors to compute anomaly scores under the short-term and long-term windows.

Existing studies on time-series anomaly detection have shown that adaptive window strategies can better match varying temporal patterns and improve detection performance [51–53]. Building on this observation, an adaptive sliding window adjustment mechanism is introduced to adjust window lengths according to the volatility of anomaly scores.

Let $w_s(t)$ and $w_l(t)$ denote the short-term and long-term window lengths at time t, with corresponding anomaly scores $Z_s(t)$ and $Z_l(t)$. The anomaly score sequences within the windows are

$$\{Z_s(t-w_s(t)),\dots,Z_s(t-1)\} \quad \text{and} \quad \{Z_l(t-w_l(t)),\dots,Z_l(t-1)\}.$$

The volatility of anomaly scores within each window is measured by the variance

$$\sigma_s(t) = \mathrm{Var}\big(Z_s(t-w_s(t)),\dots,Z_s(t-1)\big), \qquad \sigma_l(t) = \mathrm{Var}\big(Z_l(t-w_l(t)),\dots,Z_l(t-1)\big). \tag{10}$$

Following the strategy adopted in adaptive detection frameworks [54], two thresholds τ_h and τ_l are introduced to control the adjustment of window lengths. When the volatility exceeds τ_h, the window length is reduced to enhance sensitivity to abrupt anomalies. When the volatility falls below τ_l, the window length is increased to capture more stable structural trends.

The update rules for the sliding windows are defined as

$$w_s(t+1) = \begin{cases} \max(w_{s,\min},\, w_s(t)-1), & \sigma_s(t) > \tau_h, \\ \min(w_{s,\max},\, w_s(t)+1), & \sigma_s(t) < \tau_l, \\ w_s(t), & \text{otherwise}, \end{cases} \tag{11}$$

$$w_l(t+1) = \begin{cases} \max(w_{l,\min},\, w_l(t)-1), & \sigma_l(t) > \tau_h, \\ \min(w_{l,\max},\, w_l(t)+1), & \sigma_l(t) < \tau_l, \\ w_l(t), & \text{otherwise}, \end{cases} \tag{12}$$

where $w_{s,\min}$, $w_{s,\max}$, $w_{l,\min}$, and $w_{l,\max}$ denote the lower and upper bounds of the allowable window lengths.

4.5. Anomalous time point determination

After the adaptive mechanisms determine the spectral dimensionality and the lengths of the short-term and long-term windows, this section further aggregates the multi-view anomaly scoring functions to obtain a robust final anomaly score and accurately identify the most significant anomalous time points.

Following the methodology in [35], we aggregate the two perspectives by taking their maximum value, $Z_t = \max\big(Z_s(t),\ Z_l(t)\big)$. This procedure produces a temporal sequence of anomaly scores $\{Z_1, Z_2, \ldots, Z_T\}$. In dynamic networks, anomalies often manifest as abrupt changes, such as structural breakdowns, sudden reversals of information flow, or functional shifts of core nodes. These disruptions typically lead to significant deviations in spectral features between consecutive time steps. To capture such variations more sensitively, we further apply a differencing operation to the anomaly score sequence. The rationale is to assess whether the current change is more pronounced than the previous, namely, not only requiring the anomaly score at the current step to be high, but also that its increase over the prior step is substantial. Formally, the differenced sequence is expressed as

$$Z_t^* = \max(Z_t - Z_{t-1}, 0) \tag{13}$$

Finally, the most significant anomaly is identified by selecting the time step corresponding to $\max\{Z_1^*, Z_2^*, \ldots, Z_T^*\}$, which represents the maximum refined anomaly score in the sequence [35].

5. Experiments and results

To evaluate the effectiveness and robustness of the proposed H-GAD method, we conduct extensive experiments on both synthetic and real-world directed dynamic graph datasets.

5.1. Experimental setup

The experiments are organized into two main parts: synthetic experiments and real-world experiments.

5.1.1. Datasets

We evaluate the proposed method on both synthetic and real-world directed dynamic graph datasets. The synthetic datasets are generated using the stochastic block model (SBM), which allows us to simulate controlled structural perturbations and evaluate detection performance under different settings. The real-world experiments are conducted on two representative datasets: the UCI Message network and a global vaccine trade network.

5.1.2. Baselines

To enable a fair performance comparison, we compare the proposed method H-GAD with the following baselines:

LAD. [35] This method detects change points based on the Laplacian matrix and singular value decomposition (SVD), where network embeddings are derived from the Laplacian representation. Two sliding-window sizes are employed to capture both short-term and long-term temporal properties, enabling detection of structural anomalies in dynamic graphs. However, it relies on the conventional Laplacian matrix, which implicitly assumes symmetric relationships between nodes. As a result, it does not explicitly distinguish between in-degree and out-degree patterns, and may fail to capture anomalies arising from asymmetric or directional structural variations.

TENSORSPLAT. [33] This method models dynamic networks as higher-order tensors, where structural and temporal information are jointly encoded. It then applies CP decomposition to extract low-rank latent factors along the temporal dimension. Anomaly detection is subsequently performed on these factors to identify change points and anomalous patterns in network evolution. While effective in capturing global temporal patterns, it does not explicitly preserve directional node-to-node relationships, and therefore may overlook anomalies driven by asymmetric interactions or directional changes.

Fréchet. [36] This method maps each network snapshot to a symmetric positive definite (SPD) matrix derived from the graph Laplacian and characterizes temporal variations via sliding-window Fréchet statistics. Although applicable to dynamic networks, it relies on symmetric matrix representations to construct SPD matrices, which do not explicitly encode edge directionality. Consequently, directional dependencies are not preserved, limiting its ability to detect anomalies arising from asymmetric interactions or directional flow changes.

Overall, these methods do not explicitly model edge directionality, which limits their ability to capture anomalies driven by asymmetric interactions. This limitation motivates the proposed H-GAD framework.

5.1.3. Evaluation metric

For quantitative assessment, we employ the Hits at n ($H@n$) metric, which measures the proportion of true anomaly events that appear among the top-n time points ranked by predicted anomaly score. Concretely, known event timestamps in each real dataset are treated as ground-truth anomalies; detection effectiveness is then assessed by the degree to which these ground-truth events are recovered within the top-n predictions returned by each method.

Table 1
Community numbers at different change points under the pure setting.

Time point	Community change
0	$N_c = 2$
10	$N_c = 4$
15	$N_c = 10$
30	$N_c = 2$
60	$N_c = 4$
75	$N_c = 10$
115	$N_c = 2$

Table 2
Performance comparison with baseline methods under the pure setting.

Dataset	Metric	H-GAD (Proposed)	LAD	TENSORSPLAT	Fréchet
Pure Synthetic	Hits@6	**100%**	16.7%	16.7%	66.7%

5.2. Synthetic experiments

To evaluate the performance of H-GAD and examine its behavior under different network structural settings, we construct synthetic datasets based on the Stochastic Block Model (SBM) [55]. By adjusting parameters such as the number of communities and the probabilities of intra and inter-community connections, the SBM can flexibly simulate structural mutations and event occurrences in networks, thereby providing a controllable environment for assessing anomaly detection methods.

5.2.1. Pure setting

In the synthetic experiments, a temporal directed weighted network is generated using the stochastic block model (SBM). The network sequence contains 151 time steps, where each snapshot consists of 500 nodes with community structures. In this setting, only the number of communities (N_c) varies, while all other parameters remain fixed. The intra-community and inter-community connection probabilities are set to $p_{in} = 0.25$ and $p_{ex} = 0.05$, respectively, and edge weights are uniformly sampled from the interval $[1, 10]$.

Change points are introduced by modifying the community structure at specific time steps, where the number of communities switches to 2, 4, and 10, as summarized in Table 1. After each change point, the network remains stable until the next structural transition.

Between change points, the network evolves from the previous snapshot through random edge perturbations with rate $\alpha = 0.1$, simulating gradual structural variations. The generated network sequence therefore contains both abrupt structural changes and stable evolutionary periods, providing a controlled environment for evaluating change-point detection methods. All snapshots are stored as edge lists, where each edge records its timestamp, endpoints, and weight.

The proposed method employs an adaptive mechanism to dynamically determine the optimal feature dimensionality over the entire spectral space and to adjust the sliding-window lengths according to the fluctuation characteristics of the anomaly scores. As a result, the selected parameters are $k = 456$, the short-term window length $w_s = 5$, and the long-term window length $w_l = 10$. Under this parameter configuration, the anomaly score sequence produced by H-GAD is illustrated in Fig. 2. It can be observed that, among the 6 injected change points, H-GAD successfully detects all 6. A quantitative comparison of baseline performances is reported in Table 2.

5.2.2. Hybrid setting

While the pure setting evaluates the sensitivity of H-GAD to abrupt community structure changes, real-world dynamic networks often exhibit both structural shifts and gradual variations in connection strength. To evaluate the robustness of H-GAD under more complex dynamics, a hybrid setting incorporating both change points and events is designed.

In this setting, both the number of communities (N_c) and the connection probabilities (p_{in}, p_{ex}) in the stochastic block model (SBM) vary over time. Change points are generated by modifying the number of communities (e.g., from 2 to 4 or 10), representing abrupt structural transitions. Events are simulated by adjusting the connection probabilities (e.g., reducing p_{in} from 0.250 to 0.237) while keeping the community structure unchanged.

Consistent with the pure setting, the generated network sequence contains 151 time steps, with each snapshot consisting of 500 nodes and edge weights uniformly distributed in $[1, 10]$. During periods without events or change points, the network evolves from the previous snapshot through random edge perturbations with rate $\alpha = 0.1$.

In the experimental design, events are injected at $T = 10, 30$, and 75, while change points occur at $T = 15, 60$, and 115, with the initial state defined at $T = 0$. The corresponding variations in community numbers and connection probabilities are summarized in Table 3. The resulting sequence contains both abrupt structural transitions and gradual variations in connection strength.

In this mixed-data experiment, the feature dimensionality automatically determined by the adaptive mechanism is $k = 456$, with a short-term window length of $w_s = 5$ and a long-term window length of $w_l = 10$. Under this parameter configuration, the anomaly

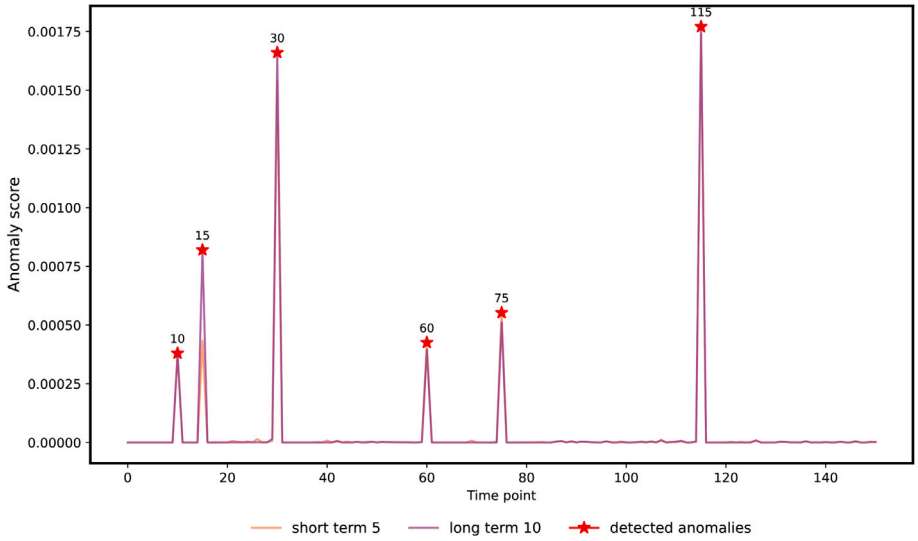

Fig. 2. H-GAD correctly detects all six injected change points, with each anomaly corresponding to abrupt structural perturbations and yielding prominent peaks in the anomaly score sequence.

Table 3
Community numbers and connection probabilities at different time steps under the hybrid setting.

Time point	Type	Community change	Connection probability change
0	Start point	$N_c = 2$	$p_{in} = 0.250,\ p_{ex} = 0.050$
10	Event	$N_c = 2$	$p_{in} = 0.237,\ p_{ex} = 0.040$
15	Change point	$N_c = 4$	$p_{in} = 0.250,\ p_{ex} = 0.050$
30	Event	$N_c = 4$	$p_{in} = 0.238,\ p_{ex} = 0.048$
60	Change point	$N_c = 10$	$p_{in} = 0.250,\ p_{ex} = 0.050$
75	Event	$N_c = 10$	$p_{in} = 0.247,\ p_{ex} = 0.050$
115	Change point	$N_c = 2$	$p_{in} = 0.250,\ p_{ex} = 0.050$

Table 4
Performance comparison with baseline methods under the hybrid setting.

Dataset	Metric	H-GAD (Proposed)	LAD	TENSORSPLAT	Fréchet
Hybrid Synthetic	Hits@6	**66.7%**	0%	0%	66.7%

scores predicted by H-GAD are shown in Fig. 3. The experimental results indicate that, among the 3 injected structural change points and 3 event anomalies, H-GAD is able to accurately detect abrupt changes in community structure, while also effectively identifying anomaly events induced by variations in connection probabilities. A quantitative comparison of baseline performances is reported in Table 4.

5.3. Real-world experiments

To further evaluate the effectiveness of the proposed Hermitian Laplacian spectral anomaly detection method (H-GAD), experiments are conducted on two real-world directed dynamic graph datasets: the UCI Message network and a global vaccine trade network. These datasets represent different application domains and exhibit clear directional interaction patterns.

5.3.1. UCI Message network

The UCI dataset originates from an online student community at the University of California, Irvine. A directed weighted dynamic graph is constructed where nodes represent users and directed edges denote message transmissions. Edge weights correspond to the total number of characters sent between two users within a day. The dataset contains 1899 users and spans from April 2004 to October 2004, producing 196 daily snapshots. Each edge (i, j, w) indicates that user i sent w characters to user j on that day. To ensure numerical stability in spectral analysis, a self-loop with weight 1 is added to each node.

Based on the temporal characteristics of the dataset, the UCI Message network exhibits clear weekly interaction patterns. Under the proposed adaptive mechanism, the short-term and long-term window lengths are determined as 7 days and 14 days, respectively, which are consistent with the weekly communication cycle observed in the dataset. Based on the cumulative spectral energy

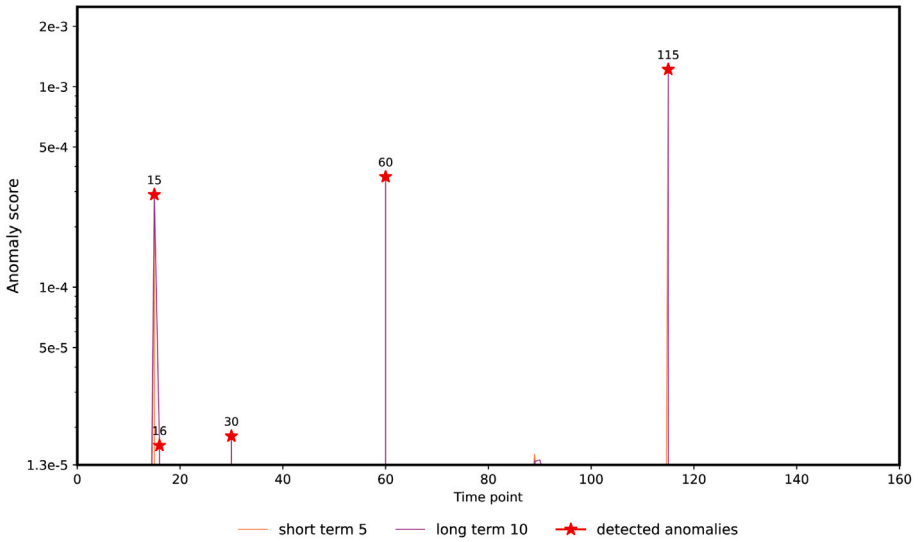

Fig. 3. H-GAD detects four of the six anomalous time points, with higher anomaly scores assigned to more significant structural changes, reflecting its sensitivity to pronounced structural variations.

distribution, the feature dimensionality is automatically selected as $k = 27$, where the leading eigenvalues are used to construct the spectral representation at each time step.

Panzarasa [56] reported that Day 65 corresponds to the end of the spring semester, while Day 158 marks the beginning of the fall semester. Therefore, we focus on these two known abnormal time points: Day 65 (end of spring semester) and Day 158 (beginning of fall semester). Both points are associated with pronounced structural transitions and shifts in interaction patterns within the network. To quantitatively evaluate anomaly detection performance, we adopt the Hits@2 metric, which assesses whether the top two detected anomalies coincide with the ground-truth abnormal events.

The results are presented in Fig. 4. The results indicate that H-GAD successfully detected Day 65 as an anomaly. This anomaly achieved the highest score across the entire sequence, demonstrating H-GAD's superior capability in modeling global structural patterns and capturing directional sensitivity. From a structural perspective, this anomaly is associated with a reduction in outgoing message interactions from active users, leading to a more sparse and less interconnected communication pattern. In particular, the imbalance between sending and receiving activities becomes more pronounced, reflecting a directional weakening of information flow across the network. These findings confirm the advantages of H-GAD in detecting structure-altering anomalies driven by directionality in dynamic graphs, particularly in identifying boundary events of periodic phenomena (e.g., semester transitions) that exhibit distinct anomalous patterns.

5.3.2. Global vaccine trade network

This dataset records monthly vaccine trade flows among countries from May 2017 to December 2023. A directed weighted temporal graph is constructed, where nodes represent countries or regions and edges denote vaccine exports between them. Edge weights correspond to exported vaccine quantities (in kilograms). The dataset spans 80 months, resulting in a sequence of 80 graph snapshots.

Based on the temporal dynamics of the dataset, the global vaccine trade network exhibits seasonal patterns. Using the adaptive mechanism, the short-term and long-term window lengths are selected as 3 months and 6 months, respectively, which are consistent with common international trade and procurement cycles. The spectral dimensionality is determined as $k = 14$ according to the cumulative spectral energy criterion.

To evaluate anomaly detection performance, we focus on key real-world events that significantly impacted global vaccine trade. The following time points are identified as major structural anomalies:

August 2020 represents an important structural turning point in the global vaccine trade network, during which several major international initiatives reshaped vaccine cooperation and procurement mechanisms. The COVAX initiative experienced a rapid expansion in participation, with 172 countries and economies expressing interest in joining the facility by August 2020. As a global platform for vaccine procurement and distribution, the expansion of COVAX introduced new cooperative relationships and supply agreements among countries, leading to the emergence of new nodes and cross-national trade links in the network. At the same time, early vaccine production capacity and supply arrangements were determined during this period [57,58]. Therefore, August 2020 can be regarded as a structural anomaly point in the global vaccine trade network.

Another key time point occurred on November 11, 2020, when the European Commission signed a large-scale vaccine procurement agreement with Pfizer–BioNTech on behalf of the European Union. This agreement represented one of the earliest multinational vaccine procurement contracts and marked the first centralized large-scale procurement within the global vaccine

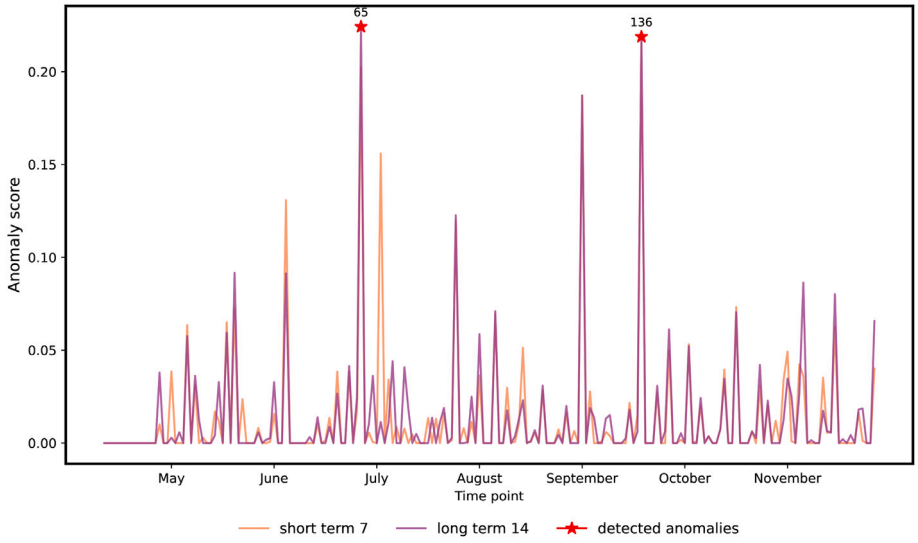

Fig. 4. H-GAD correctly detects Day 65, corresponding to the end of the spring semester, achieving the highest anomaly score in the UCI Message network dataset.

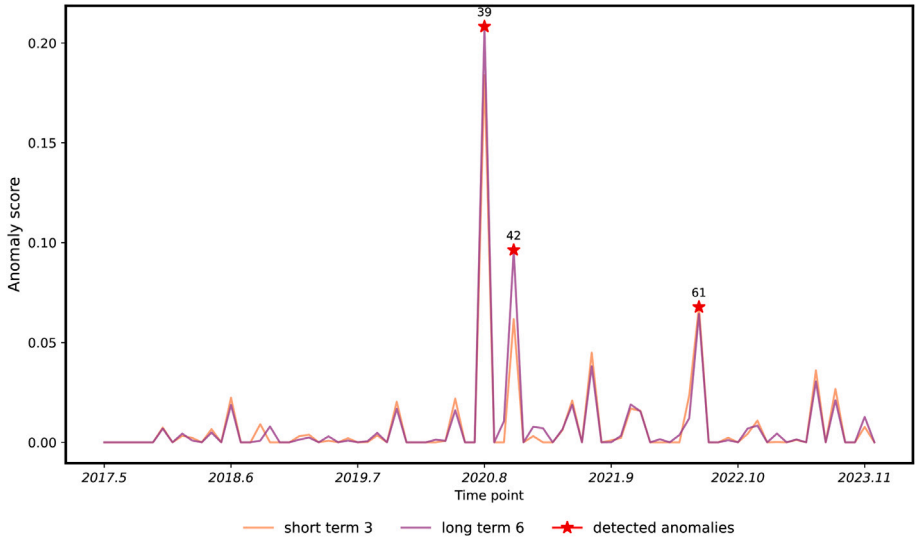

Fig. 5. H-GAD correctly detects August 2020, November 2020, and June 2022 as the top three time points with the highest anomaly scores.

distribution system [59,60]. The agreement significantly strengthened cross-national coordination and supply-chain organization in vaccine distribution, making November 2020 another structural anomaly point in the network. Meanwhile, the global pandemic remained severe during this period, further intensifying international demand for vaccine cooperation [61–64].

June 2022 marks another important stage in the evolution of the global vaccine trade network. During this period, the World Trade Organization adopted the TRIPS waiver, several countries initiated localized vaccine manufacturing programs, and the European Union introduced new vaccine distribution mechanisms. These institutional adjustments substantially affected international vaccine trade relationships and cross-regional connectivity, making June 2022 another anomaly point in the network [65].

In this experiment, we adopt Hits@4 as the evaluation metric, which measures whether the top four anomaly scores in the detection results cover the true anomaly points. The results are presented in Fig. 5.

These results demonstrate that H-GAD successfully identifies the 39th time point (August 2020), the 42nd time point (November 2020), and the 61st time point (June 2022), highlighting its superior sensitivity and discriminative capability in handling dynamic graphs characterized by pronounced directionality (e.g., abrupt changes in vaccine flows between exporting and importing countries) and structural perturbations (e.g., the emergence of new nodes or disruptions in cross-border trade).

From a structural perspective, the detected anomaly at the 39th time point (August 2020) can be interpreted as a directional reorganization of trade relationships. During this period, several major exporting countries appear to have increased their outgoing

Table 5
Performance comparison with baseline methods on real-world datasets.

Method	UCI (Hits@2)	Global vaccine trade network (Hits@4)
H-GAD (Proposed)	**50%**	**100%**
LAD	0%	0%
TENSORSPLAT	0%	66.7%
Fréchet	0%	0%

Table 6
AUC values under different threshold values τ for four datasets.

τ	Pure	Hybrid	UCI	VAC
0.80	0.6649	0.5339	0.5515	0.9957
0.82	0.6626	0.5339	0.5515	0.9957
0.85	0.6615	0.5356	0.5464	1.0000
0.88	0.6603	0.5397	0.5438	1.0000
0.90	0.6626	0.5425	0.5412	1.0000
0.93	0.6678	0.5454	0.5438	1.0000
0.95	0.6741	0.5477	0.5438	1.0000

connections, forming new directed trade links toward regions that previously exhibited relatively weak import activity. At the same time, the distribution of incoming flows becomes less balanced, indicating a transition from relatively distributed trade patterns to more concentrated export–import structures.

These changes are reflected not only in the magnitude of trade volumes, but also in the redistribution of directional connectivity across the network. Such directional shifts lead to noticeable variations in the Hermitian Laplacian spectrum, which explains why the proposed method successfully identifies this anomaly. Similar structural patterns can also be observed at the other detected anomaly points, although with different intensities.

The baseline comparison results are reported in Table 5. The results obtained from two real-world directed dynamic network datasets demonstrate that the proposed H-GAD method consistently outperforms the baseline approaches in terms of anomaly detection performance. Overall, H-GAD demonstrates stable and superior performance in identifying key anomalous events across diverse real-world network scenarios, reflecting enhanced robustness and generalization ability. This advantage primarily stems from its explicit modeling of edge directionality within a spectral analysis framework, which enables higher sensitivity and reliability in detecting structural disruptions and anomalous behaviors during the evolution of real directed networks.

5.4. Sensitivity analysis of the eigenvalue energy threshold

To evaluate the robustness of the adaptive feature dimensionality selection mechanism, a parameter sensitivity analysis is conducted on the eigenvalue energy threshold τ. The anomaly detection performance is measured using the Area Under the Curve (AUC) on four datasets: *pure*, *hybrid*, *UCI*, and *VAC*. By varying τ and recording the corresponding AUC scores, we examine the influence of the energy coverage threshold on detection performance and assess the stability of the commonly used setting $\tau = 0.95$ across different datasets.

The AUC metric is used to evaluate the anomaly detection performance. AUC measures the model's ability to distinguish anomalous samples from normal ones based on the Receiver Operating Characteristic (ROC) curve, which characterizes the trade-off between the true positive rate (TPR) and the false positive rate (FPR). Higher AUC values indicate stronger anomaly discrimination capability. The mathematical formulation of AUC is given as follows:

$$\mathrm{AUC} = \int_0^1 \mathrm{TPR}\left(\mathrm{FPR}^{-1}(t)\right) dt. \tag{14}$$

To further examine the influence of the threshold τ on model performance, we conduct experiments on each of the four datasets by varying τ within the range $\tau \in [0.80, 0.95]$ with a step size of 0.01. The corresponding AUC values are computed for each setting, and the results are summarized in Table 6.

As illustrated in Fig. 6, the AUC performance of the four datasets exhibits different trends under varying τ values, reflecting differences in anomalous structural characteristics and spectral separability. For the UCI dataset, the AUC fluctuates by less than 0.01 within $\tau \in [0.80, 0.95]$, indicating stable performance that is largely insensitive to the threshold. A slight improvement is observed when $\tau \geq 0.94$, suggesting that retaining additional spectral energy can enhance anomaly representation. The VAC dataset shows similar stability despite containing burst-type anomalies, where the AUC consistently remains above 0.995 and reaches 1.000 within $\tau = 0.83$–0.95, indicating that its anomalous structures are strongly identifiable in the spectral domain.

In contrast, the synthetic *pure* and *hybrid* datasets exhibit a clear increasing trend in AUC as τ grows, particularly when $\tau \geq 0.92$. This suggests that for structural mutations and composite anomalies, higher energy coverage helps preserve critical structural variations and improves anomaly detection performance. Overall, real-world datasets remain stable across a relatively wide range of τ, whereas synthetic datasets are more sensitive to increases in the threshold. This difference can be attributed to the fact that anomalies in synthetic datasets are more structured and separable, while real-world anomalies are typically more complex and

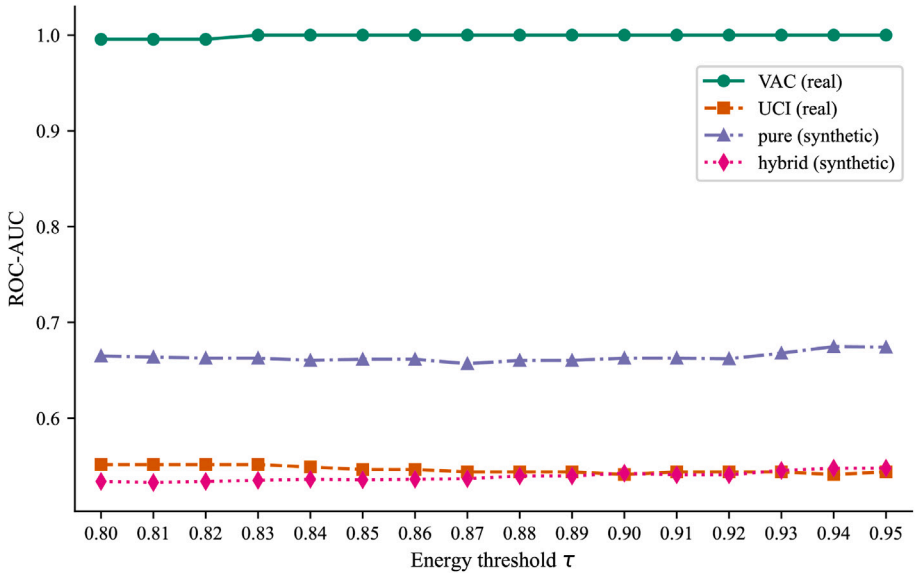

Fig. 6. Parameter sensitivity analysis under varying τ values across four datasets. Real-world datasets exhibit stable AUC performance, while synthetic datasets show increased sensitivity to τ. Based on stability and detection performance, $\tau = 0.95$ is selected as the optimal threshold for all datasets.

noisy, leading to a more dispersed spectral energy distribution. Considering stability, detection accuracy, and generalization ability, $\tau = 0.95$ achieves consistently strong performance across all four datasets and is therefore selected as the final energy coverage threshold in this study.

5.5. Analysis and validation of network structural properties at anomalous points

To validate the structural significance of the detected anomalies, we analyze the temporal evolution of key network metrics around the identified anomalous time points in both datasets. The analysis characterizes variations in connectivity intensity and structural properties associated with these events, providing an interpretable explanation of the detected anomalies.

5.5.1. UCI Message network

In the UCI Message network, the structural characteristics of the detected anomaly are examined through the temporal evolution of representative topological metrics. Specifically, average weighted degree is considered to characterize global structural variations, while the weighted average path length is further analyzed in the time window surrounding the anomalous point to capture local structural changes. The results are shown in Fig. 7.

The average weighted degree reflects the mean interaction intensity among users, measured by the average number of message characters sent or received by each node. As illustrated in Fig. 7(a), the average weighted degree exhibits a clear declining trend at day 65, indicating a substantial reduction in interaction intensity among users. This time point coincides with the end of the spring semester, during which user activity decreases significantly, leading to a marked drop in overall connectivity strength.

To further examine the structural variation around the anomaly on day 65, we analyze local structural properties, namely weighted average path length, within the window from day 62 to day 68. The weighted average path length describes the efficiency of information transmission in the network. As shown in Fig. 7(b), the path length remains low and stable prior to day 65, indicating efficient communication through short paths [66]. When the anomaly occurs, the path length increases sharply, implying that many direct communication links disappear and information must traverse longer paths. After the anomaly, the path length decreases but does not fully return to its previous level.

Taken together, the anomaly is characterized by a simultaneous decrease in connectivity intensity and deterioration in structural efficiency. This indicates a transition from a densely connected and efficient communication network to a more sparse and less efficient structure. These observations provide clear evidence that the detected anomaly corresponds to a significant structural disruption, thereby supporting the effectiveness of the proposed H-GAD method.

5.5.2. Global vaccine trade network

Based on the Hermitian Laplacian spectral analysis, three anomalous time points — August 2020, November 2020, and June 2022 — are identified in the global vaccine trade network. To further assess the reliability of these detections, we examine the temporal evolution of network structural characteristics in the global vaccine trade network.

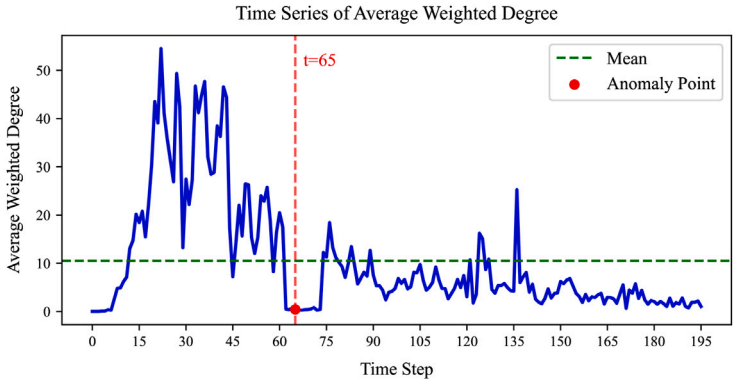

(a) Average Weighted Degree.

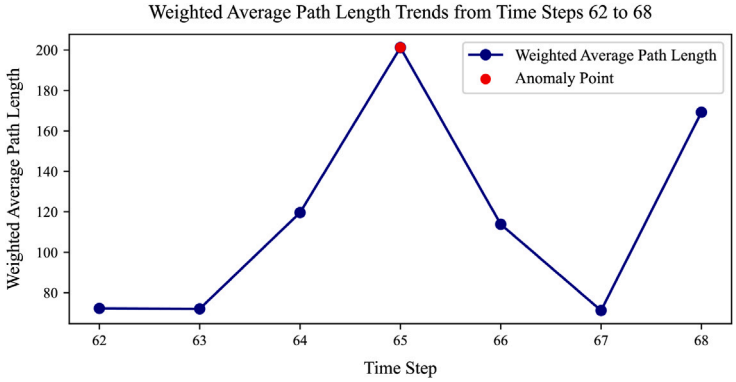

(b) Weighted Average Path Length.

Fig. 7. Temporal evolution of key network metrics in the UCI Message network. The average weighted degree and weighted average path length characterize connectivity intensity and structural efficiency, respectively. A pronounced decrease in average weighted degree and a simultaneous increase in path length are observed at the anomalous time point (day 65), indicating a transition from a densely connected and efficient structure to a sparse and less efficient network.

The average weighted degree is adopted as the primary structural indicator to characterize variations in connectivity intensity, where nodes represent countries or regions and edge weights correspond to vaccine trade volumes. Higher values indicate stronger trade interactions and greater structural cohesion in the global trade system. To identify structural deviations in the temporal evolution of this metric, a CUSUM (Cumulative Sum) control chart is employed. The CUSUM method, originally proposed by Page in 1954 [67], detects structural changes by accumulating deviations from a reference value, thereby amplifying persistent shifts in the data. In the analysis, both the positive cumulative sum (C^+) and negative cumulative sum (C^-) are computed. The statistic C^+ captures sustained upward deviations, whereas C^- reflects sustained downward trends. An anomaly is identified when the absolute value of either statistic exceeds a predefined control limit. In this study, the control limit is set to five times the standard deviation of the average weighted degree, and any cumulative deviation beyond this threshold is regarded as a significant structural anomaly. As illustrated in Fig. 8, which summarizes the temporal evolution of the metric and the corresponding CUSUM analysis.

Fig. 8(a) shows that from 2017 to early 2020, the average weighted degree fluctuates slightly around its mean, indicating a relatively stable trade structure with moderate variations in trade intensity. However, three pronounced peaks appear in August 2020, November 2020, and June 2022, suggesting periods of intensified connectivity and structural adjustment in the global vaccine trade network. The first peak in August 2020 coincides with the rapid expansion of the COVAX initiative, which attracted participation from 172 countries and economies amid the accelerating global spread of COVID-19. During this period, vaccines begins to transition into essential global public goods, stimulating cross-border trade in vaccine-related materials and strengthening international supply links. The second peak in November 2020 corresponds to the large-scale procurement agreement between the European Union and Pfizer and the subsequent expansion of vaccine production and international distribution. The third peak in June 2022 reflects a further structural transition in the global vaccine trade system, during which institutional adjustments and expanded manufacturing capacity contributed to renewed growth in trade connectivity.

As illustrated in Fig. 8(b), the CUSUM control chart further confirms these deviations. The positive cumulative sum (C^+) increases sharply at the identified anomalous time points and exceeds the upper control limit, while the negative cumulative sum (C^-) remains

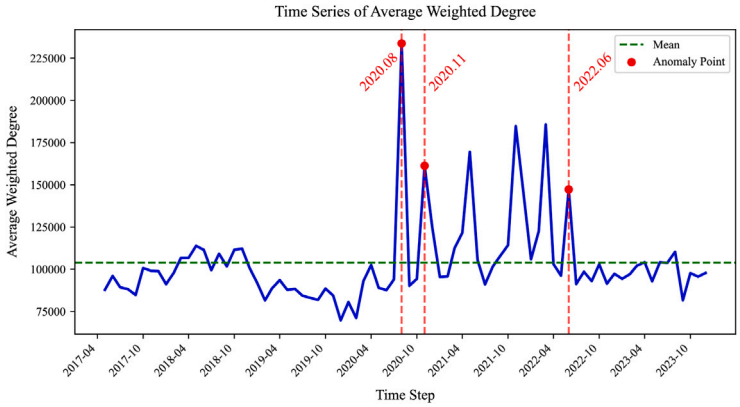

(a) Three anomaly points in August 2020, November 2020, and June 2022.

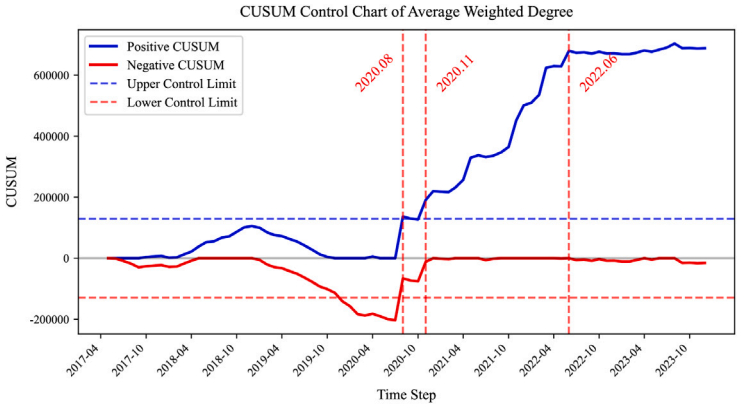

(b) CUSUM control chart of the average weighted degree, indicating structural anomalies at detected time points.

Fig. 8. Global structural analysis of the vaccine trade network. The network exhibits three distinct structural peaks corresponding to major global events, with the CUSUM analysis confirming significant upward deviations in connectivity, indicative of temporal reorganization and intensification of trade relations.

Table 7
Statistical test results for structural changes.

Metric	Test statistic (U)	p-value	Conclusion
Average weighted degree	6.0000	0.0006	Significant difference detected

relatively stable. This pattern indicates sustained upward deviations in connectivity intensity and confirms that the observed peaks correspond to significant structural changes rather than random fluctuations.

To statistically assess the significance of these structural deviations, a Mann–Whitney U nonparametric test is applied to the average weighted degree. The test compares the anomalous time points (August 2020, November 2020, and June 2022) with the remaining observations. As reported in Table 7, the test yields a statistic of $U = 6.0000$ with a p-value of 0.0006, which is below the significance level $\alpha = 0.05$. These results indicate a significant difference between the anomaly group and the reference group, thereby confirming the structural significance of the detected anomalies.

In summary, the detected time points correspond to clear structural shifts in the global vaccine trade network. The peaks in average weighted degree, together with the CUSUM results and statistical test, indicate significant increases in connectivity intensity. These findings support the effectiveness of the H-GAD framework in identifying meaningful structural anomalies in dynamic trade networks.

6. Conclusion

This study examined anomaly detection in directed dynamic graphs and introduced a spectral framework based on the Hermitian Laplacian matrix. By constructing the Hermitian adjacency matrix and its associated Laplacian operator, the proposed method

preserves directional structural information while tracking the spectral evolution of dynamic networks over time. A dual-window temporal framework was further incorporated to jointly capture short-term fluctuations and long-term dependencies, and the resulting spectral variations were used to define an anomaly score for identifying structurally abnormal time points.

Experiments on synthetic networks generated by the stochastic block model, together with two real-world datasets — the UCI Message network and the global vaccine trade network — demonstrated the effectiveness of the proposed approach. In particular, the method consistently achieved strong performance in terms of the Hits@n metric and accurately identified key anomalous time points associated with substantial structural disruptions. Complementary global and local structural analyses further supported the reliability and interpretability of the detected anomalies.

Overall, the results show that explicitly incorporating edge directionality into spectral analysis can substantially improve anomaly detection in dynamic graph settings. The proposed framework therefore offers a useful and interpretable tool for studying structural perturbations in directed temporal networks. Future work may extend this framework to weighted or multilayer directed graphs, explore online detection settings, and investigate its applicability to a broader range of complex real-world systems.

CRediT authorship contribution statement

Guihai Yu: Writing – original draft, Validation, Resources, Project administration, Methodology, Funding acquisition, Formal analysis. **Yulei Yue:** Writing – original draft, Visualization, Validation, Supervision, Software, Methodology, Investigation, Formal analysis, Data curation, Conceptualization. **Xiaopeng Li:** Writing – review & editing, Validation, Supervision, Resources, Project administration, Methodology, Funding acquisition, Formal analysis. **Matjaž Perc:** Writing – review & editing, Resources, Project administration, Investigation, Funding acquisition, Formal analysis.

Declaration of competing interest

The authors declare that they have no known competing financial interests or personal relationships that could have appeared to influence the work reported in this paper.

Acknowledgments

This work is partly supported by the National Natural Science Foundation of China (NSFC) (Grant Nos. 62363004 and 12461062); Guizhou Provincial Basic Research Program (Natural Science) (Grant No. MS[2025]232); Natural Science Foundation of Guizhou (Grant Nos. [2020]1Z001 and [2021]5609). This work was also supported by the Open Fund of Guizhou Key Laboratory of Artificial Intelligence and Brain-inspired Computing (Grant No. AILKF20250106). In addition, M.P. is supported by the Slovenian Research and Innovation Agency (Javna agencija za znanstvenoraziskovalno in inovacijsko dejavnost Republike Slovenije) (Grant No. P1-0403).

Data availability

The code and data that support the findings of the study are available from the corresponding author upon reasonable request.

References

[1] Akoglu L, Faloutsos C. Anomaly, event, and fraud detection in large network datasets. In: Proceedings of the sixth ACM international conference on web search and data mining. 2013, p. 773–4.
[2] Ra D, Lee D, Lee S. Language model-driven anomaly detection and interpretation in chaotic signals via temporal-dynamics-aware embedding. Chaos Solitons Fractals 2026;208:118157.
[3] Gupta M, Gao J, Aggarwal CC, Han J. Outlier detection for temporal data: A survey. IEEE Trans Knowl Data Eng 2013;26(9):2250–67.
[4] Ranshous S, Shen S, Koutra D, Harenberg S, Faloutsos C, Samatova NF. Anomaly detection in dynamic networks: A survey. Wiley Interdiscip Rev Comput Stat 2015;7(3):223–47.
[5] Li S, Pandey A, Hooi B, Faloutsos C, Pileggi L. Dynamic graph-based anomaly detection in the electrical grid. IEEE Trans Power Syst 2021;37(5):3408–22.
[6] Li G, Jung JJ. Dynamic graph embedding-based anomaly detection on internet of things time series. Expert Syst 2024;41(2):e13083.
[7] Saheed YK, Misra S. CPS-IoT-PPDNN: A new explainable privacy preserving DNN for resilient anomaly detection in cyber-physical systems-enabled IoT networks. Chaos Solitons Fractals 2025;191:115939.
[8] Kei YL, Li H, Chen Y, Padilla OHM. Change point detection on a separable model for dynamic networks. 2023, Preprint arXiv:2303.17642.
[9] Dey A, Kumar BR, Das B, Ghoshal AK. Outlier detection in social networks leveraging community structure. Inf Sci 2023;634:578–86.
[10] Elliott A, Cucuringu M, Luaces MM, Reidy P, Reinert G. Anomaly detection in networks with application to financial transaction networks. 2019, Preprint arXiv:1901.00402.
[11] Tang T, Yao J, Wang Y, Sha Q, Feng H, Xu Z. Application of deep generative models for anomaly detection in complex financial transactions. In: Proceedings of the international conference on artificial intelligence and internet of digital economy. 2025, p. 133–7.
[12] Li K, Yu Y, Hu W, Cui Y, Li J. Robust asymmetric nonnegative matrix factorization for community detection in directed network. Chaos Solitons Fractals 2025;200:117144.
[13] Li X, Zhen X, Qi X, Han H, Zhang L, Han Z. Dynamic community detection based on graph convolutional networks and contrastive learning. Chaos Solitons Fractals 2023;176:114157.
[14] Xu J, Hu H, Ellison G, Yu L, Whalen CC, Liu L. Bayesian estimation of transmission networks for infectious diseases. J Math Biol 2025;90(3):29.
[15] Wong WK, Moore A, Cooper G, Wagner M. What's strange about recent events (WSARE): An algorithm for early detection of disease outbreaks. J Mach Learn Res 2005;6:1961–98.

[16] Yu G, Jiao Y, Li X, Perc M. DI-CCNS: Directed community detection via co-clustering and node similarity with adaptive parameter optimization. Chaos Solitons Fractals 2025;199:116631.
[17] Yu G, Jiao Y, Dehmer M, Emmert-Streib F. Community detection in directed networks based on network embeddings. Chaos Solitons Fractals 2024;189:115630.
[18] Smaha S. Haystack: An intrusion detection system. In: Proceedings of the aerospace computer security applications conference. 1988, p. 37–44.
[19] Bremer R. Outliers in statistical data. Technometrics 1995;37(1):117–8.
[20] Basseville M, Nikiforov IV. Detection of abrupt changes: Theory and applications. Englewood Cliffs: Prentice-Hall; 1993.
[21] Breunig MM, Kriegel HP, Ng RT, Sander J. LOF: Identifying density-based local outliers. In: Proceedings of the ACM SIGMOD international conference on management of data. 2000. p. 93–104.
[22] Knorr EM, Ng RT, Tucakov V. Distance-based outliers: Algorithms and applications. VLDB J 2000;8(3):237–53.
[23] Lu B, Liu W. Nonuniform clustering of wireless sensor network node positioning anomaly detection and calibration. J Sens 2021;2021:5733308.
[24] Gan G. A k-means algorithm with automatic outlier detection. Electron 2025;14(9):1723.
[25] Murtagh F. A survey of recent advances in hierarchical clustering algorithms. Comput J 1983;26(4):354–9.
[26] Jain AK, Dubes RC. Algorithms for clustering data. Englewood Cliffs: Prentice-Hall; 1988.
[27] Müllner D. Modern hierarchical agglomerative clustering algorithms. 2011, Preprint arXiv:1109.2378.
[28] Ester M, Kriegel HP, Sander J, Xu X. A density-based algorithm for discovering clusters in large spatial databases with noise. In: Proceedings of the ACM SIGKDD international conference on knowledge discovery and data mining. 1996, p. 226–31.
[29] Wang W, Yang J, Muntz RR. STING: A statistical information grid approach to spatial data mining. In: Proceedings of the international conference on very large data bases. 1997.
[30] Breiman L, Friedman J, Olshen RA, Stone CJ. Classification and regression trees. New York: Chapman & Hall/CRC; 1984.
[31] Markou M, Singh S. Novelty detection: A review. Signal Process 2003;83(12):2481–97.
[32] Liu FT, Ting KM, Zhou ZH. Isolation forest. In: Proceedings of the IEEE international conference on data mining. 2008, p. 413–22.
[33] Koutra D, Papalexakis EE, Faloutsos C. TensorSplat: Spotting latent anomalies in time. In: Proceedings of the panhellenic conference on informatics. 2012, p. 144–9.
[34] Koutra D, Shah N, Vogelstein JT, Gallagher B, Faloutsos C. DeltaCon: Principled massive-graph similarity function with attribution. ACM Trans Knowl Discov Data 2016;10(3).
[35] Huang S, Hitti Y, Rabusseau G, Rabbany R. Laplacian change point detection for dynamic graphs. In: Proceedings of the 26th ACM SIGKDD international conference on knowledge discovery & data mining. 2020, p. 349–58.
[36] Luo R, Krishnamurthy V. Fréchet-statistics-based change point detection in dynamic social networks. IEEE Trans Comput Soc Syst 2023;11(2):2863–71.
[37] Cucuringu M, Li H, Sun H, Zanetti L. Hermitian matrices for clustering directed graphs: Insights and applications. In: Proceedings of the international conference on artificial intelligence and statistics. 2020, p. 983–92.
[38] Mohar B. Hermitian adjacency spectrum and switching equivalence of mixed graphs. Linear Algebra Appl 2016;489:324–40.
[39] Yu G, Dehmer M, Emmert-Streib F, Jodlbauer H. Hermitian normalized Laplacian matrix for directed networks. Inf Sci 2019;495:175–84.
[40] Sulem D, Kenlay H, Cucuringu M, Dong X. Graph similarity learning for change-point detection in dynamic networks. Mach Learn 2024;113(1).
[41] Yu G, Kang Y, Li X, Perc M, Završnik J. Evolution of global healthcare trade networks: Structural fracture detection, topological responses, and cross-commodity dependency restructuring. Chaos Solitons Fractals 2026;202:117474.
[42] Wang Y, Chakrabarti A, Sivakoff D, Parthasarathy S. Fast change point detection on dynamic social networks. 2017, Preprint arXiv:1705.07325.
[43] Hu Y, Qu A, Work D. Detecting extreme traffic events via a context-augmented graph autoencoder. ACM Trans Intell Syst Technol 2022;13(6).
[44] Yu G, Liu X, Qu H. Singularity of Hermitian Laplacian matrix of mixed graphs. Appl Math Comput 2017;293:287–92.
[45] Furutani S, Shibahara T, Akiyama M, Hato K, Aida M. Graph signal processing for directed graphs based on the Hermitian Laplacian. In: Proceedings of the European conference on machine learning and knowledge discovery in databases. 2019, p. 447–63.
[46] Humbert P, Le Bars B, Oudre L, Kalogeratos A, Vayatis N. Learning Laplacian matrix from graph signals with sparse spectral representation. J Mach Learn Res 2021;22.
[47] Jolliffe IT. Principal component analysis. New York: John Wiley & Sons; 1986.
[48] Jolliffe IT, Cadima J. Principal component analysis: A review and recent developments. Philos Trans A Math Phys Eng Sci 2016;374:20150202.
[49] Idé T, Kashima H. Eigenspace-based anomaly detection in computer systems. In: Proceedings of the ACM SIGKDD international conference on knowledge discovery and data mining. 2004, p. 440–9.
[50] Golub GH, Reinsch C. Singular value decomposition and least squares solutions. Linear Algebra Appl 1971;14:134–51.
[51] Aminikhanghahi S, Cook DJ. A survey of methods for time series change point detection. Knowl Inf Syst 2017;51(2):339–67.
[52] Truong C, Oudre L, Vayatis N. Selective review of offline change point detection methods. Signal Process 2019;167:107299.
[53] Dimoudis D, Vafeiadis T, Nizamis A, Ioannidis D, Tzovaras D. Adaptive rolling median methodology for time series anomaly detection. Procedia Comput Sci 2023;217:584–93.
[54] Guo M, Chen C, Hou C, Wu Y, Yuan X. SWAM: Adaptive sliding window and memory-augmented attention model for rumor detection. In: Proceedings of the empirical methods in natural language processing conference. 2025, p. 14430–41.
[55] Holland PW, Laskey KB, Leinhardt S. Stochastic blockmodels: First steps. Soc Netw 1983;5(2):109–37.
[56] Panzarasa P, Opsahl T, Carley KM. Patterns and dynamics of users' behavior and interaction in online communities. J Am Soc Inf Sci Technol 2009;60(5):911–32.
[57] World Health Organization. 172 countries and multiple candidate vaccines engaged in COVID-19 vaccine global access facility. 2020, https://www.who.int/news/item/24-08-2020-172-countries-and-multiple-candidate-vaccines-engaged-in-covid-19-vaccine-global-access-facility.
[58] Gavi, the Vaccine Alliance. Up to 100 million COVID-19 vaccine doses to be made available for low- and middle-income countries as early as 2021. 2020, https://www.gavi.org/news/media-room/100-million-covid-19-vaccine-doses-available-low-and-middle-income-countries-2021.
[59] Al Jazeera. Covid-19 cases still surging in the Americas, WHO warns. 2020, https://www.aljazeera.com/news/2020/11/11/covid-19-cases-still-surging-in-the-americas-who-warns.
[60] Callaway E. Covid vaccine excitement builds as Moderna reports third positive result. Nat 2020;587:337–8.
[61] World Health Organization. WHO COVID-19 dashboard. 2020, https://data.who.int/dashboards/covid19/cases.
[62] Al Jazeera. Global coronavirus death toll hits 800, 000: live news. 2020, https://www.aljazeera.com/news/2020/8/22/global-coronavirus-death-toll-hits-800000-live-news.
[63] The Guardian. Bars and shops closed as Europe battles second wave of coronavirus. 2020, https://www.theguardian.com/world/2020/nov/15/bars-and-borders-stay-closed-as-europe-battles-second-wave-of-coronavirus.
[64] The New Yorker. The pandemic's winter surge is here. 2020, https://www.newyorker.com/science/medical-dispatch/the-pandemics-winter-surge-is-here.
[65] World Trade Organization. WTO issues updated note on trade in medical goods in the context of tackling COVID-19. 2022, https://www.wto.org/english/news_e/news22_e/covid_20jul22_e.htm.
[66] Sun X, Liu Z, Perc M. Effects of coupling strength and network topology on signal detection in small-world neuronal networks. Nonlinear Dynam 2019;96(3):2145–55.
[67] Page ES. Continuous inspection schemes. Biom 1954;41(1–2):100–15.